

# The Electromagnetic Imaging Calorimeter of PAMELA

V. Bonvicini<sup>1</sup>, G. Barbiellini<sup>1</sup>, M. Boezio<sup>1</sup>, E. Mocchiutti<sup>1</sup>, P. Schiavon<sup>1</sup>, G. Scian<sup>1</sup>, A. Vacchi<sup>1</sup>, G. Zampa<sup>1</sup>, N. Zampa<sup>1</sup>, D. Bergström<sup>2</sup>, P. Carlson<sup>2</sup>, T. Francke<sup>2</sup>, J. Lund<sup>2</sup>, M. Pearce<sup>2</sup>, M. Hof<sup>3</sup>, W. Menn<sup>3</sup>, M. Simon<sup>3</sup>, S. A. Stephens<sup>4</sup>, M. Ambriola<sup>5</sup>, R. Bellotti<sup>5</sup>, F. Cafagna<sup>5</sup>, F. Ciaccio<sup>5</sup>, M. Circella<sup>5</sup>, C. De Marzo<sup>5</sup>, N. Giglietto<sup>5</sup>, B. Marangelli<sup>5</sup>, N. Mirizzi<sup>5</sup>, P. Spinelli<sup>5</sup>, O. Adriani<sup>6</sup>, M. Boscherini<sup>6</sup>, R. D'Alessandro<sup>6</sup>, N. Finetti<sup>6</sup>, M. Grandi<sup>6</sup>, P. Papini<sup>6</sup>, A. Perego<sup>6</sup>, S. Piccardi<sup>6</sup>, P. Spillantini<sup>6</sup>, E. Vannuccini<sup>6</sup>, P.S. Bartalucci<sup>7</sup>, L. Marino<sup>7</sup>, M. Ricci<sup>7</sup>, M. Casolino<sup>8</sup>, M.P. De Pascale<sup>8</sup>, G. Furano<sup>8</sup>, A. Morselli<sup>8</sup>, P. Picozza<sup>8</sup>, R. Sparvoli<sup>8</sup>, L.M. Barbier<sup>9</sup>, E.R. Christian<sup>9</sup>, J.F. Krizmanic<sup>9</sup>, J.W. Mitchell<sup>9</sup>, J.F. Ormes<sup>9</sup>, R.E. Streitmatter<sup>9</sup>, U. Bravar<sup>10</sup>, and S.J. Stochaj<sup>10</sup>, S. Bertazzoni<sup>11</sup>, A. Salsano<sup>11</sup>, G. Bazilevskaia<sup>12</sup>, A. Grigorjeva<sup>12</sup>, R. Mukhametshin<sup>12</sup>, Y. Stozhokov<sup>12</sup>, E. Bogomolov<sup>13</sup>, S. Krutkov<sup>13</sup>, G. Vasiljev<sup>13</sup>, A.M. Galper<sup>14</sup>, S.V. Koldashov<sup>14</sup>, M.G. Korotkov<sup>14</sup>, V.V. Mikhailov<sup>14</sup>, A.A. Moiseev<sup>14</sup>, J.V. Ozerov<sup>14</sup>, S.A. Voronov<sup>14</sup>, Y. Yurkin<sup>14</sup>, G. Castellini<sup>15</sup>, A. Gabbanini<sup>15</sup>, F. Taccetti<sup>15</sup>, M. Tesi<sup>15</sup>, V. Vignoli<sup>15</sup>

<sup>1</sup>*Dipartimento di Fisica dell'Università and Sezione INFN di Trieste, Via A. Valerio 2, I-34147 Trieste, Italy*

<sup>2</sup>*Royal Institute of Technology (KTH), S-104 05 Stockholm, Sweden*

<sup>3</sup>*Universität Siegen, 57068 Siegen, Germany*

<sup>4</sup>*Tata Institute of Fundamental Research, Bombay 400 005, India*

<sup>5</sup>*Dipartimento di Fisica dell'Università and Sezione INFN di Bari, Via Amendola 173, I-70126 Bari, Italy*

<sup>6</sup>*Dipartimento di Fisica dell'Università and Sezione INFN di Firenze, Largo Enrico Fermi 2, I-50125 Firenze, Italy*

<sup>7</sup>*Laboratori Nazionali INFN, Via Enrico Fermi 40, CP 13, I-00044 Frascati, Italy*

<sup>8</sup>*Dipartimento di Fisica dell'Università and Sezione INFN di Roma, Tor Vergata, Via della Ricerca Scientifica 1, I-00133 Roma, Italy*

<sup>9</sup>*Code 661, NASA/Goddard Space Flight Center, Greenbelt, MD 20771, USA*

<sup>10</sup>*Box 3-PAL, New Mexico State University, Las Cruces, NM 88003, USA*

<sup>11</sup>*Electronic Engineering Department, Tor Vergata, Via della Ricerca Scientifica 1, I-00133 Roma, Italy*

<sup>12</sup>*Lebedev Physical Institute, Russia*

<sup>13</sup>*Ioffe Physical Technical Institute, Russia*

<sup>14</sup>*Moscow Engineering and Physics Institute, Moscow, Russia*

<sup>15</sup>*Istituto di Ricerca Onde Elettromagnetiche CNR, Firenze, Italy*

## ABSTRACT

The PAMELA imaging calorimeter is a sampling calorimeter made of silicon sensor planes interleaved with plates of tungsten absorber. The calorimeter is intended to perform a precise measurement of the total energy deposited, to reconstruct the spatial development of the showers (both in the longitudinal and in the transverse directions), and to measure the energy distribution along the shower itself.

Within the PAMELA apparatus, the main physics task of the imaging calorimeter is to take part in the extraction of the antiproton signal from the large electron background (with an efficiency of about 90% and a rejection power of about  $10^{-4}$ ) and in the identification of positrons in a vast background of protons (with an efficiency of about 90% and a rejection power better than  $10^{-4}$ ). Besides these items, the calorimeter will also be employed to measure an interesting new channel, the study of very high (1 TeV and above) energy electrons.

We report on the instrument design details, the simulated performance and the first experimental results from test beam data.

## Introduction

The PAMELA experiment (The PAMELA Collaboration, 1999) is a part of the Russian Italian Mission (RIM) program, which foresees several space missions with different scientific objectives. The first of these missions (RIM-1 experiment), studied the isotopic composition of cosmic nuclei by means of the silicon telescope NINA (Bakaldin et al. 1997), carried by the Russian polar orbit satellite Resource-04. The NINA instrument was launched from Bajkonur on July 10th, 1998 and has collected a significant amount of data (a twin instrument, “NINA-2”, has been also launched with success from Plesenska (Russia), on July 15th, 2000).

The PAMELA experiment (RIM-2 mission) has the scientific goal of measuring the cosmic radiation over a wide energy range. The apparatus will be installed onboard a Russian satellite of the “Resource” series and will be launched in late 2002/early 2003. Its sun-synchronous, 680 km polar orbit will allow the low energy cosmic rays to be measured while the instrument is near the poles. The main scientific objectives of PAMELA are the precise measurement of the positron flux from 50 MeV to 270 GeV and the antiproton flux from 80 MeV to 190 GeV, as well as the search for antihelium with a sensitivity of  $10^{-7}$  in the  $\overline{\text{He}}/\text{He}$  ratio.

## The Calorimeter

The calorimeter has been designed to perform a precise measurement of the total energy deposited, to reconstruct the spatial development of the shower both in the longitudinal and in the transverse direction, and to accurately measure the energy distribution along the shower itself. These measurements will facilitate the following goals:

- extraction of the antiproton signal from the large background generated by the electron flux, with an efficiency of more than 90% and a rejection power of  $10^{-4}$ ;
- identification of the positrons in the background generated by protons, with an efficiency of more than 90% and a rejection power better than  $10^{-4}$ .

## General characteristics

The PAMELA calorimeter is a sampling calorimeter made of silicon sensor planes interleaved with plates of tungsten absorber. The calorimeter has been conceived as a high granularity device. In the Z (longitudinal) direction, the granularity is determined by the thickness of the tungsten layers. Each layer is 0.26 cm thick, that is  $0.74 X_0$  (radiation lengths). The whole calorimeter is composed of 22 tungsten layers, therefore the total depth is  $16.34 X_0$  (i.e. about 0.6 interaction lengths).

The transverse granularity is given by the segmentation of the silicon detectors into 32 large strips or pads, with a pitch of 2.4 mm. Each tungsten plane is sandwiched between two layers of silicon detectors, so that the layout of a single plane is Si-X/W/Si-Y. Either view (X or Y) is composed by a square matrix of  $3 \times 3$  detectors. Each silicon detector has a surface of  $8 \times 8 \text{ cm}^2$ , hence the total sensitive area is  $24 \times 24 \text{ cm}^2$ . The total volume is  $24 \times 24 \times 18 \text{ cm}^3$ . In either view, each strip is connected to those belonging to the two detectors of the same row (or column), so that the number of electronics channels per plane is  $32 \times 3 \times 2 = 192$  and the total number of channels is  $192 \times 22 = 4224$ .

## Mechanics

The mechanical structure is based on a modular concept. The basic unit is called a “detection plane”, and it consists of an absorber plate, two PCBs (X and Y, supporting the silicon detectors and the front-end electronics up to the ADC) and the two matrices of silicon sensors. Two detection planes form a “detection module”. In a module, the two detection planes are kept together by a frame to which they are bolted at the edge of the absorber plate (Figure 1).

The 12th module is formed by two aluminium “dummy plates” (to save weight), which have the sole purpose of supporting the four read-out boards (see next section). All modules are independent and fully extractable; they are inserted like “drawers” into the main mechanical structure and then locked by a cover.

The total calorimeter mass (including electronics and cables) is 110 kg.

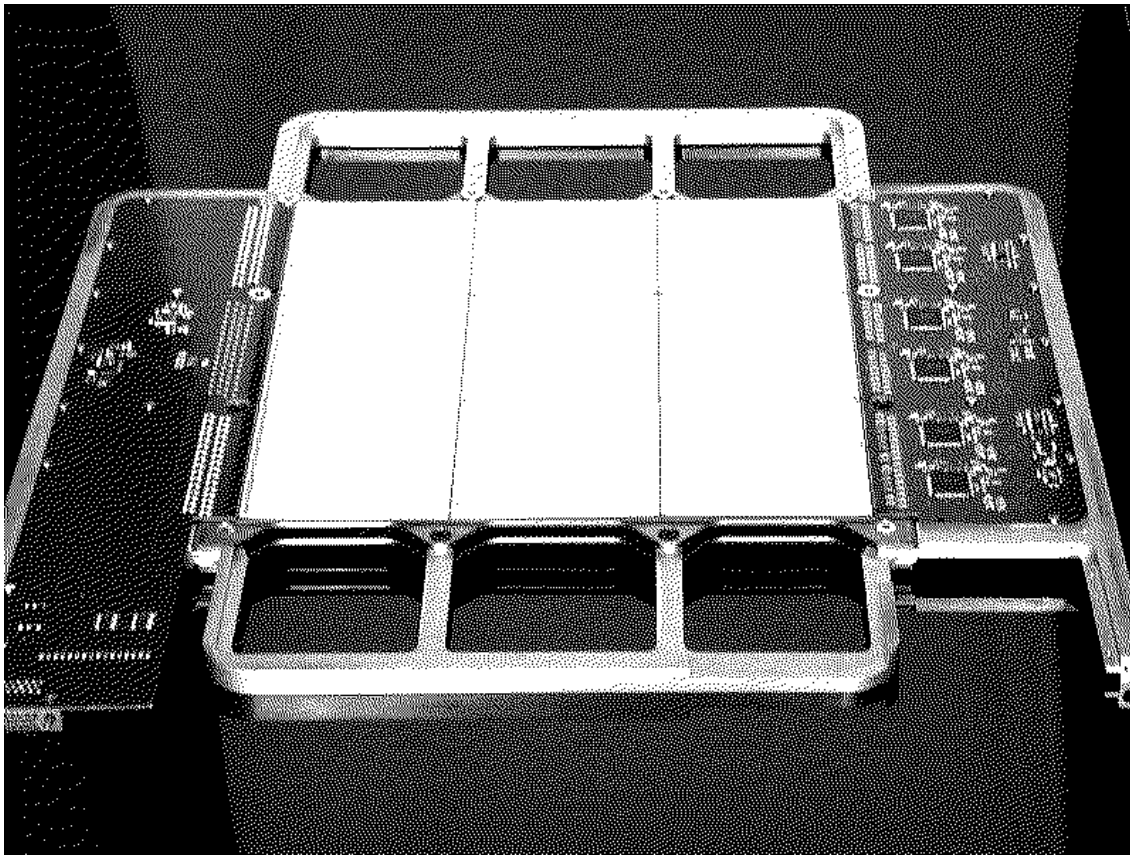


Fig. 1. Picture of one detection module of the calorimeter. The silicon detectors and front-end electronics mounted on the upper front-end board of the module are visible.

### Silicon detectors, front-end and read-out electronics.

The silicon detectors for the PAMELA calorimeter are large area devices ( $8 \times 8 \text{ cm}^2$  each),  $380 \mu\text{m}$  thick. They are fabricated on high-purity, high-resistivity ( $\geq 7 \text{ k}\Omega\text{-cm}$ ), n-type silicon substrate.

In order to avoid the use of a conductive epoxy glue for gluing the detectors onto the printed circuit boards, and therefore protecting the devices from the mechanical stress that these type of glues can induce during polymerization, the bias voltage is brought directly on the junction side of the devices via wire bonding. In this way, a non-conductive, silicic glue can be used for fixing the detectors onto the printed circuit boards.

More than 100 pre-series detectors from three manufacturers have been completely characterised in the laboratory. The test results are very positive. The average value of strip leakage current is about  $400 \text{ pA}$ , which corresponds to an average current per unit area of  $0.17 \text{ nA/cm}^2$ .

The front-end electronics is based on a VLSI ASIC specifically designed for the PAMELA calorimeter: the CR1.4P chip (Adams et al., 1999). The use of an ASIC allows a considerable weight saving and compact design with respect to the discrete preamplifiers previously used in balloon flights. The main design characteristics of this chip are the wide dynamic range (1400 minimum ionising particles,  $1 \text{ MIP} \simeq 5.1 \text{ fC}$  for  $380 \mu\text{m}$  thick silicon detectors), the ability to cope with a very large (up to  $\simeq 180 \text{ pF}$ ) detector capacitance, the good noise performance ( $\simeq 2700e^- \text{ rms} + 5 e^-/\text{pF}$ ) and the low power consumption ( $< 100 \text{ mW/chip}$ ). Each circuit has 16 channels and each channel comprises a charge sensitive preamplifier, a shaping amplifier, a track-and-hold circuit and an output multiplexer. A self-trigger system (see section “The calorimeter as a stand-alone system”) and an input calibration circuit are also integrated on chip.

In addition to the silicon detectors and the front-end electronics, the front-end boards also house the data conversion electronics. On each front-end board, the six CR1.4P outputs are connected to a 16-bit ADC via an analogue multiplexer. Figure 1 shows a complete front-end board mounted in a module.

The read-out electronics is housed into four printed circuit boards, which are mounted onto two special aluminium “dummy plates” inside the main mechanical structure. The read-out electronics has the task of collecting and analysing the data, prior to their transmission to the main CPU. The whole calorimeter is

divided, for the data read-out, into four independent sections. On each read-out board, an FPGA parallelises the ADC data and generates the multiplexer address. Four DSPs (Digital Signal Processors, one for each section of the Calorimeter), read and process the data and control the acquisition procedure.

## Test-beam results

The performance of the calorimeter has been studied with simulations developed from the experimental results of the previous balloon-flight calorimeter.

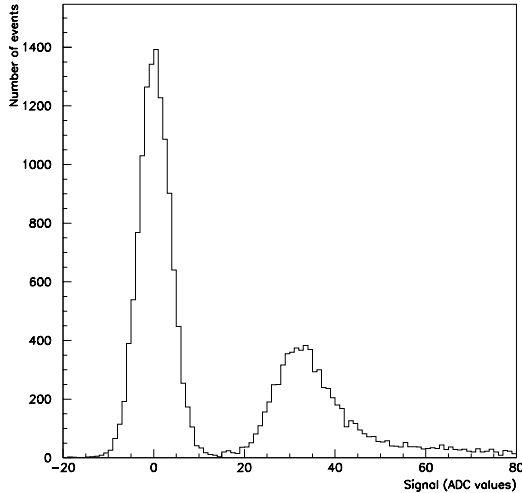


Fig. 2. Distribution of minimum ionising particle signals on one strip obtained with test beam data.

Figure 2 shows the signal distribution on one strip from minimum ionising particles (SPS data). As it can be seen, the signal is well separated from the pedestal and the most probable value of the distribution corresponds to a signal-to-noise ratio of  $9 \div 1$ , thus confirming the expected performance of the CR1.4P.

Figure 3 plots the total number of hit strips versus the total energy detected in the calorimeter. In this plot, data from different runs of pions and electrons (all at 100 GeV/c), are used. It is evident that, even with a small subset of sensitive planes such as that used in these tests, the calorimeter can effectively distinguish electrons from hadrons.

## The calorimeter as a stand-alone system

As previously described, the front-end electronics of the PAMELA calorimeter is based on the CR1.4P VLSI circuit, an analogue processor of signals from solid-state detectors specifically designed for this task. Primarily, this circuit is intended to work in synchronous mode with an external trigger signal. Nevertheless, in order to make the circuit as flexible as possible, a self-trigger system was also implemented on chip. This feature opens up the possibility to study interesting physics items.

The simulation results show that the calorimeter meets the design requirements and it is also capable of clearly identify high energy (above 100 GeV) electrons and reconstruct their energy with a resolution much better than 10%.

A partially equipped version of the calorimeter underwent a series of test-beams in May 2000 (CERN PS) and July/August 2000 (CERN SPS). The main objectives were to verify the performance of the silicon detectors and of the CR1.4P front-end chip, and to study the performance of the calorimeter (though in an uncomplete configuration), thus cross-checking the reliability of the simulations programs. The instrument was equipped with six X-type views, five of them partially equipped with only the central ladder and one fully equipped with the complete silicon detector matrix.

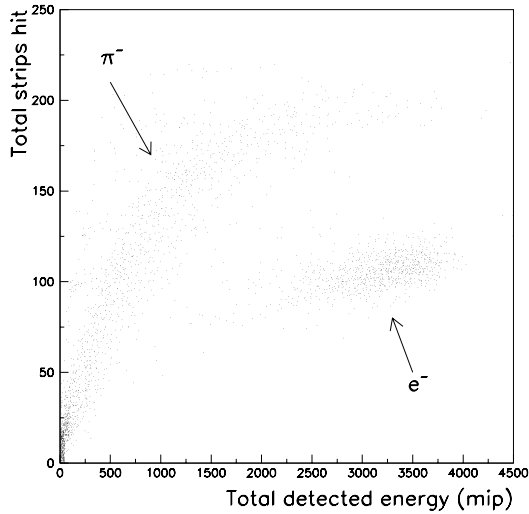


Fig. 3. Number of hit strips versus total detected energy, data from different electron and pion runs at the July/August 2000 test beam at CERN SPS.

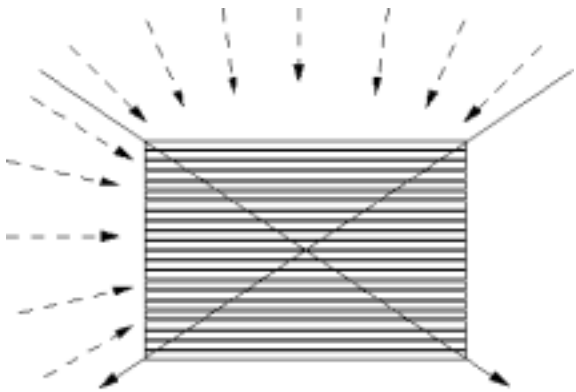


Fig. 4. Sketch of the conditions used for the simulations of the self-triggering calorimeter. Full lines: electrons, dashed lines: protons.

The simulated electron events were all required to enter the first plane and escape the last one. On the other hand, the simulations for the proton contamination were performed by accepting tracks coming from the top and one side of the structure (see Figure 4) and then extrapolating the results to the other sides (bottom side excluded). The basic idea is that a self-triggering calorimeter would be able to acquire events which release, in a defined set of planes, an energy above a given threshold.

The performance of the calorimeter in self-trigger conditions were extensively tested with Monte Carlo simulation programs, which make use of the GEANT code (Brun et al., 1993).

A complete version of the detector, identical to the one foreseen for the flight, was used in the simulations. The results are quite encouraging. For example, Figure 5 shows the energy resolution obtained for electrons with energy from 200 GeV to 1.1 TeV, with the calorimeter operating in self-trigger condition. As one can see, the energy resolution is constant at about 12% up to 700 GeV. Beyond this energy, the resolution tends to worsen (though still remaining about 16% at 1.1 TeV), due to the longitudinal leakage and to effects of

The main physics motivation to study a self-trigger system using the PAMELA Imaging Calorimeter is the possibility of measuring high-energy (from  $\approx 300$  GeV to more than 1 TeV) electrons in the cosmic ray spectra. The scientific interest of this physics channel is considerable, given the fact that up to now, only a few measurements are reported in the literature in this energy range (Nishimura et al., 1997). Since these events are quite rare in comparison with the "normal" event rate of PAMELA, it is important to have a large geometric factor in order to collect a reasonable statistics during the 3-year estimated lifetime of the mission. By accepting tracks within the volume described in Figure 4, the geometric factor would be increased by about a factor of 20 with respect to the normal acceptance of PAMELA (from  $24 \text{ cm}^2$  to  $\approx 470 \text{ cm}^2$ ).

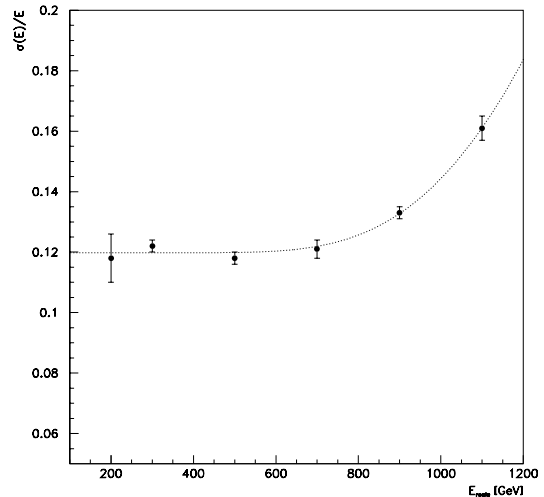


Fig. 5. Energy resolution of the calorimeter operating in self-trigger conditions for electrons.

saturation of the dynamic range of the preamplifier.

Concerning the rejection of the proton background, the simulations have shown that, in self-trigger mode, the rejection factor of the calorimeter is about 500. This value can possibly be increased by further tuning the algorithms used in the simulations.

### Conclusions and outlook

The engineering model of the PAMELA imaging calorimeter is presently under construction. A partially equipped version of the calorimeter underwent laboratory and beam tests, whose results confirm that the instrument meets all design requirements for PAMELA.

Given its design characteristics, it was also possible to study a self-triggering mode of the calorimeter, with the aim of effectively increase the statistics of PAMELA for electrons, positrons and gammas of very high energy (300 - 1000 GeV and above). Monte Carlo simulations have shown that this is indeed possible, with a proton rejection factor of about 500.

The Flight Model of the calorimeter (together with those of the other PAMELA detectors) should be completed by the end of 2001. The launch of PAMELA is foreseen in late 2002/early 2003.

### REFERENCES

- Adams, J.H., J. Ampe, G. Bashindzhagyan, V. Bonvicini, R. Kroeger, et al., The CR-1 chip: Custom VLSI Circuitry for Cosmic Rays. *Proc. 26th Int. Cosmic Ray Conf. (Salt Lake City)*, **5**, 69-71, 1999.
- Bakaldin, A., G. Barbiellini, S. Bartalucci, A. Batischev, R. Bellotti, et al., Experiment NINA: investigation of low energy nuclear fluxes in the near-Earth space, *Astrop. Phys.*, **8**, 109-121, 1997.
- Brun, R. et al., Detector Description and Simulation Tool, CERN Program Library, Geneva, 1993.
- Nishimura, J., T. Kobayashi, Y. Komori, T. Shirai, N. Tateyama and K. Yoshida, Observation of Primary Electron Spectrum and its Astrophysical Significance, *Proc. 25th Int. Cosmic Ray Conf. (Durban)*, **4**, 233-236, 1997.
- The PAMELA Collaboration, The PAMELA experiment, *Proc. 26th Int. Cosmic Ray Conf. (Salt Lake City)*, **5**, 96-99, 1999.